Experimental Study for Effect of Acceleration Frequency on the Performance in an Electrodeless Inductive Plasma Accelerator

IEPC-2017-370

Presented at the 35th International Electric Propulsion Conference
Georgia Institute of Technology • Atlanta, Georgia • USA
October 8 – 12, 2017

Kazuya Yaginuma[1] Hokuto Sekine[2], Hiroyasu Kurashige[3],
Toshihiro Matsuguma[4], Hiroyuki Koizumi[5] and Kimiya Komurasaki[6]
1 The University of Tokyo, 7-3-1 Hongo, Bunkyo-Ku, Tokyo, 113-8656, Japan

Abstract: RIPAL (Radio-frequency inductive plasma accelerator with lo-aspect ratio plasma) is one of propulsion device which is studied for a future 100 kW-class high power and full electrodeless plasma thruster. We performed the plasma flow measurement by using the asymmetry double probes, and we also calculated a plasma velocity by TOF (Time Of Flight) method. The flow speed measurement was performed with plasma generation conditions of an input power of 400 W, an exciting frequency of 13.56 MHz, a mass flow rate of 1.37 mg/s and a propellant of Xenon. We measured a signal of the asymmetry double probe during the pulsed plasma acceleration. The first peak and the second peak could be confirmed during the one cycle of the acceleration coil current. The plasma flow speed calculated from the results of TOF measurement were 28.3±3.7 km/s (f_{ac} = 31.6 kHz) and 24.8 ±6.6 km/s (f_{ac} = 49.5 kHz).

Nomenclature

e	=	amplitude of oscillation
$E_{charged}$	=	charged energy to capacitor
F	=	force
j	=	current
f_{ac}	=	frequency of acceleration coil current
$l_{p1\text{-}p2}$	=	interval length between Probe1 and Probe2
m_i	=	ion mass
M	=	mutual inductance
t	=	time
$t_{p1\text{-}1}$	=	first peak time of Probe1
$t_{p1\text{-}2}$	=	second peak time of Probe1
$t_{p2\text{-}1}$	=	first peak time of Probe2
$t_{p2\text{-}2}$	=	second peak time of Probe2
V_{ac}	=	acceleration voltage
z	=	position in z-axis direction

[1] Graduate student in the doctoral course, Dept. of Aeronautics and Astronautics, k.yaginuma@al.t.u-tokyo.ac.jp
[2] Graduate student in the master course, Dept. of Advanced Energy, h.sekine@al.t.u-tokyo.ac.jp
[3] Graduate student in the master course, Dept. of Advanced Energy, h.kurashige@al.t.u-tokyo.ac.jp
[4] Graduate student in the master course, Dept. of Aeronautics and Astronautics, t.matsuguma@al.t.u-tokyo.ac.jp
[5] Associate Prof., Dept. of Advanced Energy, koizumi@al.t.u-tokyo.ac.jp
[6] Prof., Dept. of Aeronautics and Astronautics, komurasaki@al.t.u-tokyo.ac.jp

I. Introduction

THE demand of 100 kW-class high-power electric propulsion increases year after year. The high power electric propulsion would be significant device for future manned deep space missions planned by ISECG or SpaceX. [1-2] At the current status, such high power electric propulsion has not been verified well. We could consider two major methods to achieve high power electric propulsion. One is to scale up the conventional middle-power electric propulsion. The other is to develop a new-concept electric propulsion which is suitable for such high-power class.

Conventional electric propulsions such as Hall-effect thruster and Ion thruster have achieved high-efficiency operation on a middle-power class already.[3-4] Some thrusters have a several performance records on orbit.[5-6] These conventional propulsions, however, have problems of a life time limitation by an erosion and also need a high-current cathode development. To scale up a middle-class propulsion requires a high-current cathode over 100 A and a long time duration test to confirm a decrease of a thruster performance.

On the other hand, full electrodeless electric propulsion, which does not employ a cathode or some electrodes attached plasma, has nothing to do with the cathode and erosion problem at the least. In this point, electrodeless electric propulsion is more suitable for high-power class.

Some electrodeless electric propulsions such as VASIMR, HEAT and FARAD have been studied for 100 kW-class high-power electric propulsion.[7-10] These thrusters are each high-aspect ratio shape. In these thrusters, plasma is generated in an upstream region of a tube, and accelerated in a downstream region. The feature of VASIMR's plasma acceleration is based on ion cyclotron resonance heating and magnetic nozzle acceleration. HEAT has examined several acceleration schemes, and the major acceleration is Lorentz force by using a rotating magnetic field. FARAD utilizes inductive acceleration by using a flat coil.

RIPAL (Radio frequency Inductive Plasma Accelerator with Low-aspect ratio plasma) was also proposed for one of the full-electrodeless electric propulsion.[11] RIPAL is a low-aspect ratio shape thruster. RIPAL performs plasma generation and acceleration in the same region with different RF coils. In the studies of RIPAL, the demonstration of the proposed plasma generation method and the impulse measurement have been performed already.[11,12]

The objective of this paper is to confirm the proposed acceleration procedure of RIPAL and to measure the plasma flow speed. The previous impulse measurement showed the measured impulse to energy ratio larger than the theoretical estimation only from an inductive acceleration. It would be considered that an electrothermal acceleration component was included among the actual thrust. We would like to also confirm the ratio of an electrothermal component and an inductive acceleration component by this flow speed measurement.

We measured the plasma flow speed measurement by using the asymmetry double probes and TOF (Time Of Flight) method. The plasma flow speed measurement was performed during a pulsed acceleration of a few ten μs. Two asymmetry double probes were positioned at an interval of 20 cm and moved by using the liner stage. Two types of pulsed acceleration conditions were used as a discharged current frequency of 31.6 kHz (800 mJ) and 49.5 kHz (200 mJ).

II. RIPAL

RIPAL (Radio-frequency Inductive Plasma Accelerator with Low-aspect ratio plasma) is studied for 100 kW-class high-power, full-electrodeless and inductive acceleration electric propulsion. RF-plasma is independently generated and accelerated in the same region of an insulation chamber. Generated plasma is accelerated continuously by radio frequency inductive acceleration of an applied magnetic field and an induced current within the plasma.

A. Plasma Generation

A radio-frequency plasma is a kind of plasma which could be generated in a full-electrodeless condition. A low-aspect ratio RF-plasma is chosen for the plasma source in order to decrease a power loss of the plasma generation, which is lower than a thruster of high-aspect ratio. RIPAL also employs permanent magnets for a plasma confinement in the concept.

B. Plasma Acceleration

An inductive acceleration is a kind of the acceleration schemes for electric propulsions. Plasma is accelerated by $\boldsymbol{j}\times\boldsymbol{B}$ interaction of an applied magnetic field $\boldsymbol{B}$ and an induced current $\boldsymbol{j}$ in a plasma. There have been several studies as to a plasma thruster using an inductive acceleration such as PIT (Pulsed Inductive Thruster)[13] and TWPE (Traveling

Wave Plasma Engine).[14] These thrusters have achieved to high-thrust efficiency and proved that inductive acceleration is one of the effective plasma acceleration schemes.

RIPAL also performs an inductive acceleration. In addition to this, RIPAL performs plasma generation and acceleration in the same region of insulation chamber which is a full-electrodeless condition. Schematic of operating procedure is shown in **Figure 2**.[11] When an acceleration coil current j_1 and a plasma current j_2 are induced, in a circuit model,[15] a total thrust F on plasma would be described as the below.

$$F = -j_1 j_2 \frac{\partial M}{\partial z} \tag{1}$$

The average values of F in a cycle of **Figure 2** would be larger than zero, because a mutual inductance M between j_1 and j_2 become smaller with plasma acceleration (i.e. $\partial M/\partial z < 0$). After plasma is exhausted from an insulation chamber, RIPAL immediately generates a next plasma source, and starts accelerating.

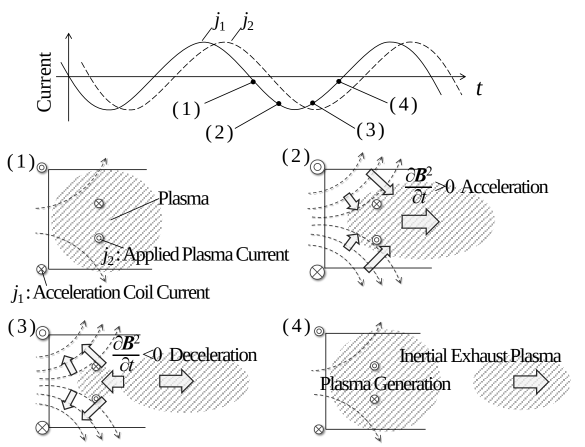

Figure 2. Schematic of operating procedure. Plasma generation and acceleration are performed independently and repeatedly in the same region of insulation chamber. j_1 is acceleration coil current and j_2 is applied plasma current. [11]

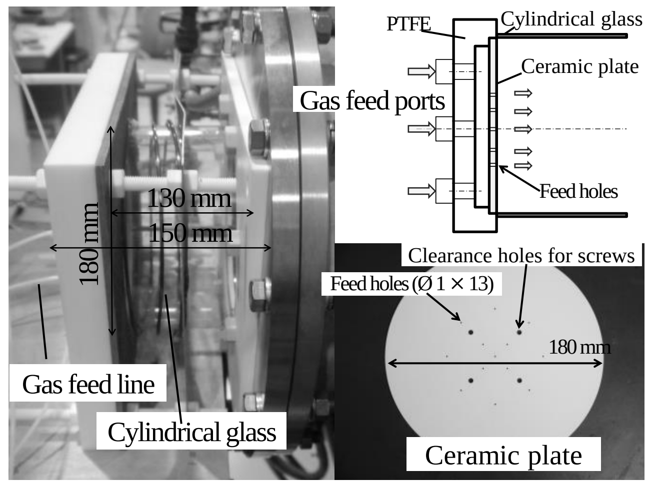

Figure 1. Experimental model of 1kW-class RIPAL connected to the vacuum chamber wall. Propellant is fed to cylindrical glass through the feed holes on the ceramic plate.

III. Experiment Equipment

C. Vacuum Chamber

The vacuum chamber (1.4 m diameter and 3.0 m length), which was pumped with one cryo pumps (12000 l/s, N2), was used in these experiments. The back pressure of the vacuum chamber was under 1.2×10^{-2} Pa (a mass flow rate of 1.37 mg/s, Xenon).

D. Experimental Model of 1 kW-class RIPAL

Experimental model of 1 kW-class RIPAL is shown on **Figure 1**. The experimental model, which was mainly consisted of cylindrical glass (Ø160 mm inner diameter and 130 mm length) and PTFE fixtures, was connected to the Ø330 mm flange of the steel vacuum chamber. Propellant gas was fed into the left-hand side of the cylindrical glass through the feed holes (1 mm diameter) of the ceramic plate shown as **Figure 1**.

E. Plasma Generation System

The type of the plasma exciting coil was loop type antenna (180 mm diameter and 3 turns) and positioned at z = 70 mm shown as **Figure 3**. Exciting coil was connected to RF power source (the frequency of 13.56 MHz) through the matching box. The range of RF input power could be changed from 0 W to 400 W.

Two type permanent magnets (cylindrical magnets of Ø60 mm×Ø32 mm×7 mm and square magnets of 20 mm×8.4 mm×4.2 mm) were used for a plasma confinement device. Cylindrical permanent magnet was positioned at the bottom of RIPAL of *z* = -20 mm. Two loops of square magnets were also positioned at each *z* = 10 mm and 120 mm shown as **Figure 3**.

F. Plasma Acceleration System

Equivalent circuit model of pulse acceleration circuit is shown on **Figure 4**. Pulse acceleration circuit was consisted of acceleration coil as an inductor, capacitor, IGBT switch and high-voltage power source. The type of the acceleration coil was flat spiral type (200 mm outside diameter, 120 mm inside diameter and 10 turns), and positioned at *z* = -20 mm shown as **Figure 3**. The switching time of IGBT switch (SEMIKRON, SKM100GB12T4) was under 200 ns. Example time history of acceleration coil current is shown on **Figure 6 (b)** (800 mJ charged energy to capacitor).

IV. Plasma Flow Measurement

Plasma flow speed measurement was performed by using two asymmetry double probes and one axis movable liner stage. Accelerated plasma flow speed was estimated by using TOF method.

G. TOF (Time Of Flight) Method

TOF (Time Of Flight) method is one of conventional methods for a flow speed measurement. In this experiment, two probes were used and positioned at an interval of 20 cm on 4 cm above from the thruster axis. Although the Mach probe method could be also be used for plasma flow speed measurement, we choose the TOF method in order to measure a pulsed accelerated plasma.

Two asymmetry double probes were used for TOF method. The asymmetry double probe consisted of two cooper plates of 20 mm×40 mm and 15 mm×15 mm. A voltage of 9.6 V was applied between the two cooper plates in order to increase the ion current flowing in the large cooper plate. Equivalent circuit model of the measurement circuit is shown on **Figure 5**. Two probes (Probe1 and Probe2) were positioned together with reference probes at an interval of 20 cm on 4 cm above from the thruster axis shown as **Figure 5**. The reference probes was electrically isolated by using a polyimide film from a plasma and its shape was the same as that of an asymmetry probe.

Figure 6 (a) shows the typical signals result of asymmetry probes during the pulsed acceleration. The signal of reference probe was included a noise from the measurement circuit. **Figure 6 (b)** shows the signals result without a plasma. A noise level of the signal without a plasma was less than 0.1 μA from the asymmetry probe during the pulse circuit discharge. In this TOF method, the first peak and the second peak after pulse acceleration circuit discharged were defined as shown in **Figure 6 (a)**. Evaluation of the first peak and

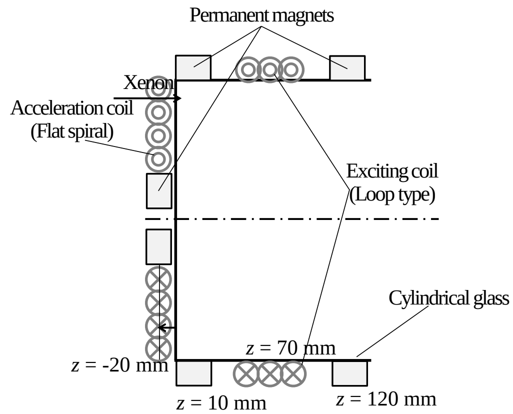

Figure 3. Experimental condition using permanent magnets. Two permanent magnets loops on the side of glass were positioned at *z* = 10 mm and *z* = 120 mm. Each magnets loop held 16 square magnets at even intervals. Exciting coil (180 mm diameter and 3 turns) was positioned at *z* = 70 mm.

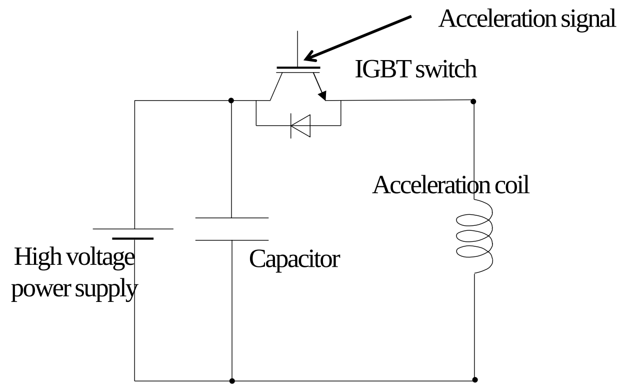

Figure 4. Equivalent circuit model of pulse acceleration circuit.

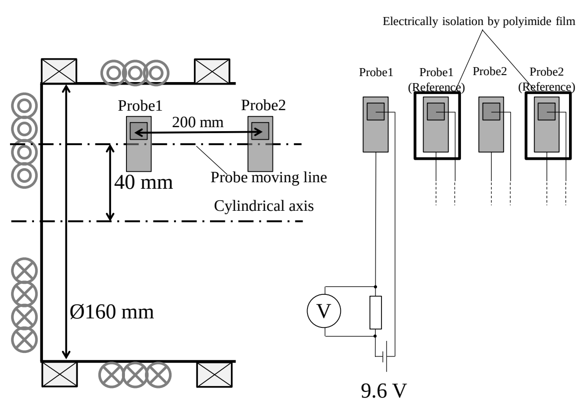

Figure 5. Schematic of the asymmetry probes position and measurement circuit. The reference probe covered with a polyimide film is electrically isolated from a plasma. Each reference probe is at the same *z* position of Probe1 and Probe2.

the second peak was performed after each signal of reference probes was subtracted from the signals of Probe1 and Probe2.

In this flow speed measurement, a plasma velocity v_p was defined as **Equation (2)**. The first peak time of Probe1 and Probe2 were presented as $t_{p1\text{-}1}$ and $t_{p2\text{-}1}$, and the interval between Probe1 and Probe2 $l_{p1\text{-}p2}$ was 20 cm.

$$v_{\rm p} = (t_{\rm p2-1} - t_{\rm p1-1})/l_{\rm p1-p2} \tag{2}$$

H. Experimental Conditions

The flow speed measurement was performed with plasma generation conditions of an input power of 400 W, a mass flow rate of 1.37 mg/s and a propellant of Xenon. Two types of pulsed acceleration conditions were used as a discharged current frequency of 31.6 kHz (800 mJ) and 49.5 kHz (200 mJ). The positions of Probe1 and Probe2 were moved at the interval of 20 mm from z=70 mm to z=230 mm by using the liner stage (**Figure 5**).

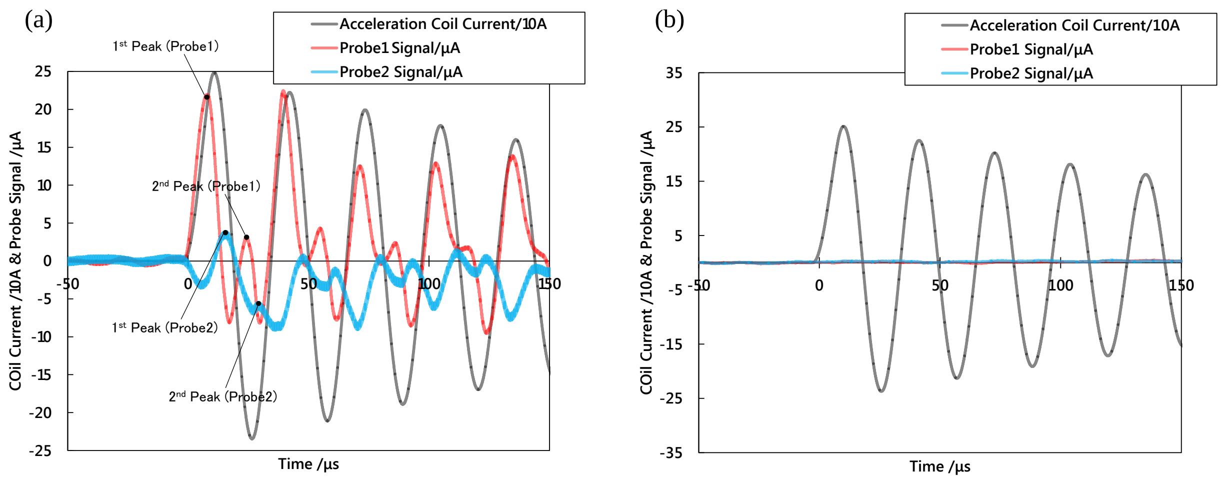

Figure 6. The results of time history of an acceleration coil current and Probe1 and Probe2 signals. Acceleration coil (200 mm outside diameter, 120 mm inside diameter and 10turns) was used. The current frequency was f_{ac} = 31.6 kHz ($E_{charged}$ = 800 mJ). (a) With plasma (a input power of 400 W, a mass flow rate of 1.37 mg/s, Xenon). The first peak and the second peak of each probe signal was defined as (a). In this graph, each peak time was calculated as $t_{p1\text{-}1}$ = 10.1 μs, $t_{p1\text{-}2}$ = 26.1 μs, $t_{p2\text{-}1}$ = 17.7 μs and $t_{p2\text{-}2}$ = 27.5 μs. (b) Without a plasma. A noise level of the signal was less than 0.1 μA shown on (b).

I. Results

The results of plasma flow measurement by TOF method are shown on **Figure 7** and **Figure 8**. **Figure 7** shows the results of an acceleration frequency of 31.6 kHz (800mJ) and **Figure 8** shows also results of an acceleration frequency of 49.5 kHz (200mJ). The calculated plasma velocities and experiment conditions are summarized on **Table 1**.

Table 1 the summary of plasma flow measurement results

Frequency of acceleration coil current: f_{ac}	31.6 kHz	49.5 kHz
Charged energy to capacitor: $E_{charged}$	800 mJ	200 mJ
The first peak time of Probe1: $t_{p1\text{-}1}$ (averaged)	10.9±0.4 μs	16.4±2.3 μs
The first peak time of Probe2: $t_{p2\text{-}1}$ (averaged)	17.9±0.9 μs	24.5±0.4 μs
Plasma velocity: v_p (averaged)	28.3±3.7 km/s	24.8±6.6 km/s

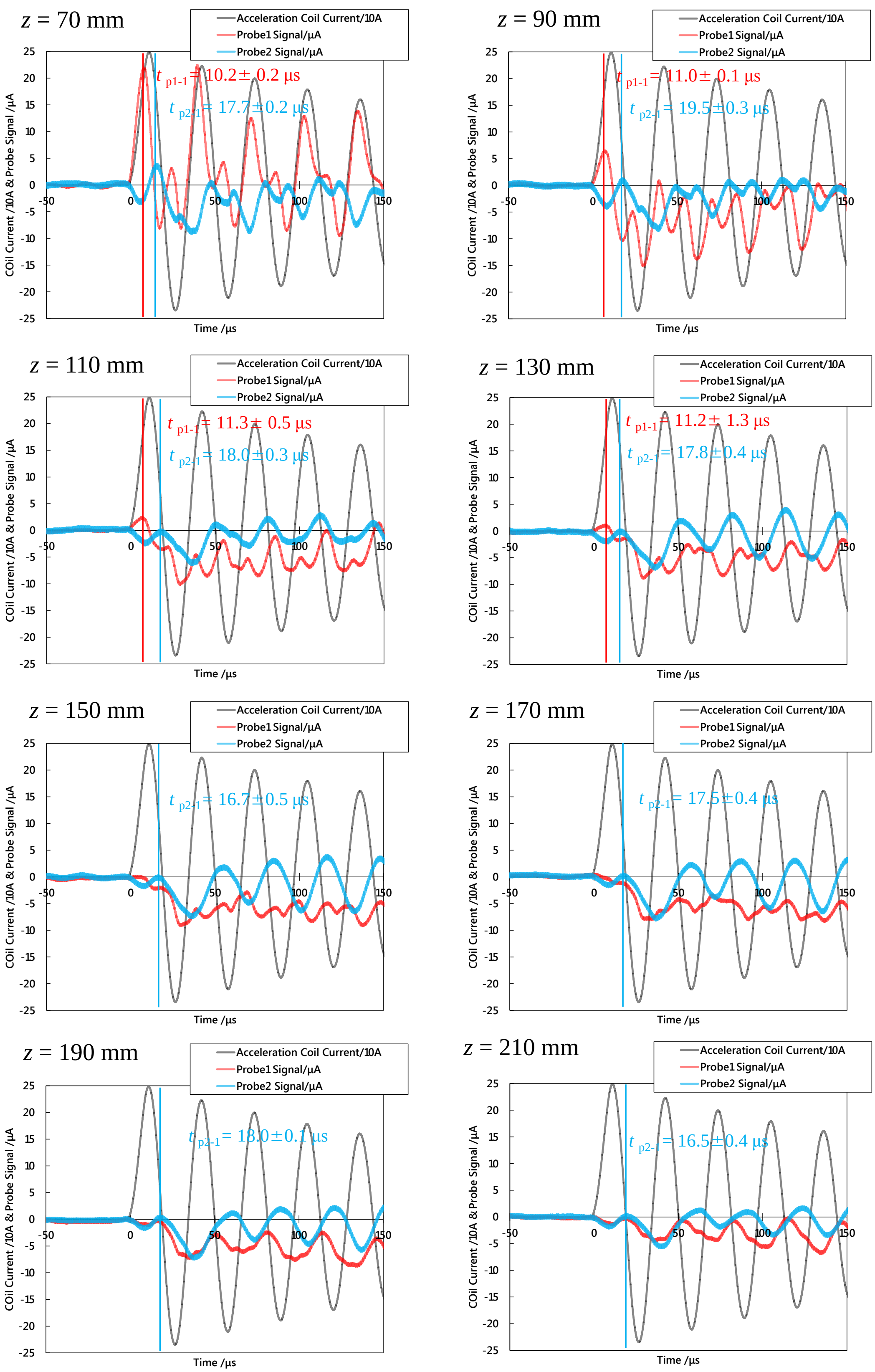

Figure 7. The results of plasma flow measurement by TOF method. The frequency of acceleration coil current was f_{ac} = 31.6 kHz (800 mJ). The position of each probe was moved at an interval of 20 mm from z=70 mm to z=210 mm. The plasma velocity could be calculated as v_p = 28.3±3.7 km/s by Equation (2). In the graph of z=150 mm, 170 mm, 190 mm and 210 mm, The first peak of Probe1 could not be defined so that the results of z=150 mm, 170 mm, 190 mm and 210 mm, was not included to the plasma velocity calculation by Equation (2).

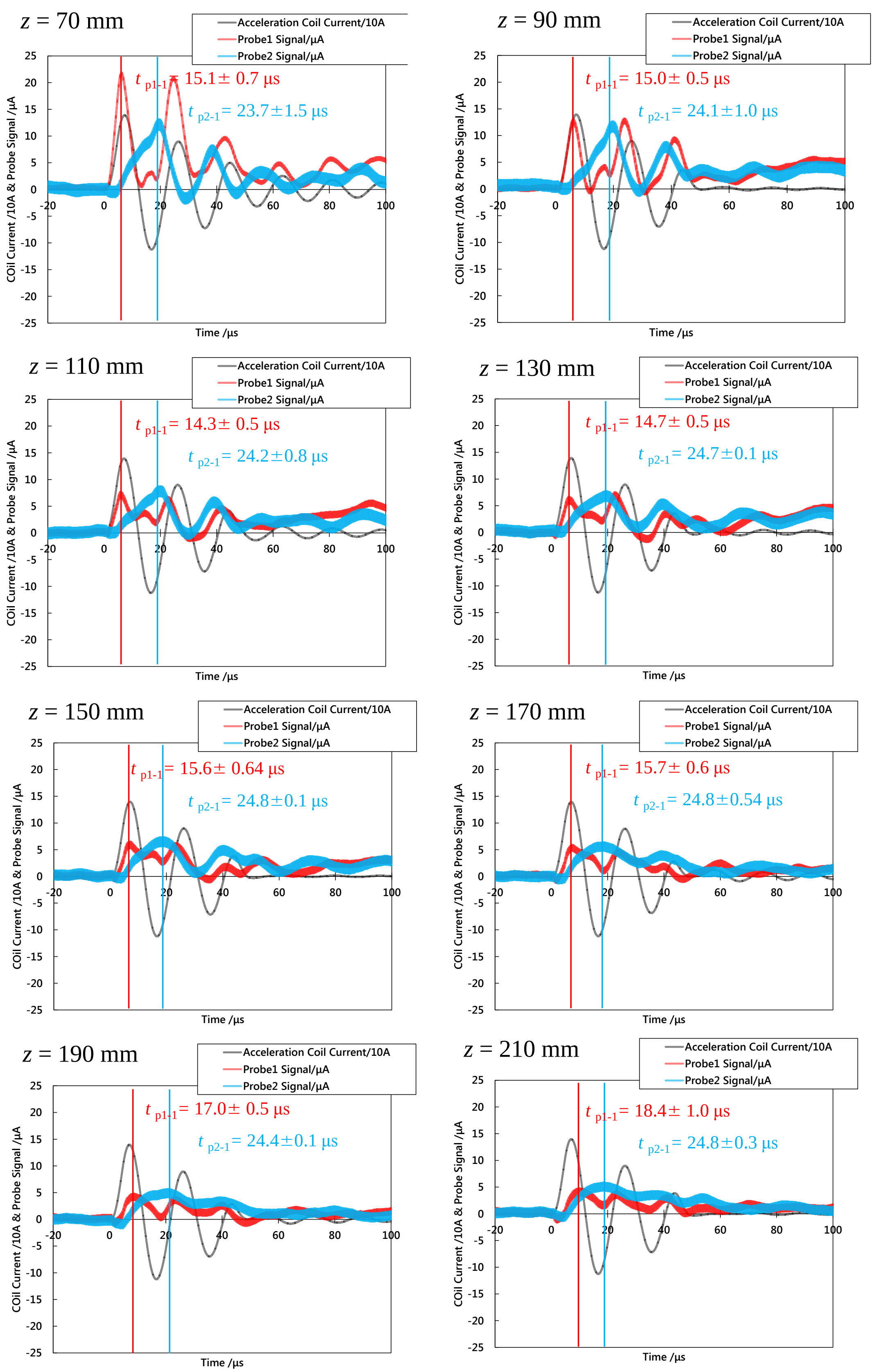

Figure 8. The results of plasma flow measurement by TOF method. The frequency of acceleration coil current was f_{ac} = 49.5 kHz (200 mJ). The position of each probe was moved at an interval of 20 mm from *z*=70 mm to *z*=210 mm. The plasma velocity could be calculated as v_p = 24.8±6.6 km/s by Equation (2).

V. Consideration

The time difference of the first peak between Probe1 and Probe2 could be confirmed shown as **Figure 7** and **Figure 8**. Because of the principle reason of the asymmetry double probes shown as **Figure 5**, a signal increasing of Probe1 and Probe2 could be considered that an ion flowing to the probe is also increasing. Then, the plasma flow velocity calculated based on **Equation (2)** would be regarded as the ion flow velocity, and an equivalent acceleration voltage of monovalent xenon ion could be calculated by using the below **Equation (3)**.

$$\frac{1}{2} m_i v_{\mathrm{p}}^2 = \mathrm{e} V_{\mathrm{ac}} \tag{3}$$

Then it could be considered that the plasma velocity v_{p} = 28.3 km/s (f_{ac} = 31.6 kHz) would be equal to V_{ac} = 543 V and v_{p} = 24.8 km/s (f_{ac} = 49.5 kHz) would be equal to V_{ac} = 417 V.

On **Figure 7** and **Figure 8**, as the probe position z became the smaller, the signal value of each probe became also the larger. It could be considered to be one reason that the acceleration coil is positioned at z = -20 mm. Compared with **Figure 7** and **Figure 8**, it could be confirmed that the peak value of the larger energy condition (E_{charged} = 800 mJ) was larger than one of the lower energy condition (E_{charged} = 200 mJ).

The first peak and the second peak could be confirmed during the one cycle of the acceleration coil current shown a **Figure 7** z = 70 mm. it could be considered that the peaks being would imply some ion acceleration by RIPAL's acceleration procedure shown as **Figure 2**.

On **Figure 7** and **Figure 8**, it could be confirmed that the waveform of each probe, which is included on the first peak and second peak exist, collapsed after the results of z=150 mm. The permanent magnets for a plasma confinement was positioned at z = 120 mm shown as **Figure 3**. After passing through the permanent magnet at the edge of the thruster glass chamber, it could be considered that a plasma is easy to diffuse in the radial direction. Furthermore, this phenomenon of the waveform collapse could be considered that it imply the phenomenon of a radial diffusion of an accelerated plasma flow, which is including some temperature.

VI. Conculsion

From the plasma flow measurement, the followings were found.

1. it could be confirmed that the proposed RIPAL's acceleration procedure would be performed during the pulsed acceleration.

2. The plasma flow speed calculated from the results of TOF measurement were 28.3±3.7 km/s (f_{ac} = 31.6 kHz) and 24.8 ±6.6 km/s (f_{ac} = 49.5 kHz).

Acknowledgments

This work was supported by JSPS KAKENHI grant: Grant-in-Aid for Challenging Exploratory Research, No. 25630387.

References

[1] ISECG, The Global Exploration Roadmap, 2013.
[2] SpaceX, Keynote Speech, International Astronautical Congress 2016.
[3] D. A. Herman, "Status of the NEXT Ion Thruster Long-Duration Test After 10,100 hr and 207 kg Demonstrated," AIAA paper 2007-5272, 2007.
[4] D. Manzella, R. Jankovsky and R. Hofer, "Laboratory Model 50 kW Hall Thruster," NASA TM-2002-211887, 2002.
[5] C. R. Koppel and F. Marchandise et al., "The SMART-1 Electric Propulsion Subsystem In Flight Experience," AIAA paper 2004-3435, 2004.
[6] J. R. Brophy et al., "Ion Propulsion System (NSTAR) DS1 Technology Validation Report," JPL Technical Report, 2001.
[7] L. D. Cassady, et al., "VASIMR Performance Results," AIAA paper 2010-6772, 2010.
[8] S. Shinohara et al., "Development of Electrodeless Plasma Thrusters With High-Density Helicon Plasma Sources," IEEE T. Plasma Sci., Vol.42, No.5, pp. 1245-1254, 2014.
[9] T. Ishii et al., "Study on electrodeless electric propulsion in high-density helicon plasma with permanent magnets," 12th Asia Pacific Physics Conf., 1 No.015047, 2014.
[10] E. Y. Choueiri and K. A. Polzin, "Faraday Acceleration with Radio-Frequency Assisted Discharge," J. Propul. Power, Vol.22 No.3, pp. 611-619, 2006.
[11] K. Yaginuma et al., "Fundamental Experiment of Radio Frequency Inductive Plasma Accelerator with Low-Aspect Ratio RF-Plasma," Journal of IAPS, Vol.23, pp. 63-68, 2016.
[12] K. Yaginuma et al., "Evaluation of Pulsed Acceleration Experiment of Radio-Frequency Inductive Plasma Accelerator with

Low-Aspect Ratio RF-Plasma," Proc. Space Transportation Symposium 2015, STEP-2015-040, 2015. (in Japanese)
[13] K. A. Polzin, "Comprehensive Review of Planar Pulsed Inductive Plasma Thruster Research and Technology," J. Propul. Power, Vol.27, No.3, pp. 513-531, 2011.
[14] L. Heflinger, S. Ridgway and A. Schaffer, "Transverse Traveling Wave Plasma Engine," AIAA J., Vol.3, pp. 1028-1033, 1965.
[15] R. G. Jahn, "Physics of Electric Propulsion," McGraw-Hill, Inc., 1996.
[16] K. Yaginuma et al., "Experimental Study for Effects of Plasma Density on the Performance in an Electrodeless Inductive Plasma Accelerator," Proc. 31st International Symposium on Space Technologies and Science, No. 2017-b-33, Ehime Japan, 2017.